

## Supplementary Material

# Improving Residential Wind Environments by Understanding the Relationship between Building Arrangements and Outdoor Regional Ventilation

Wei You, Zhi Gao, Zhi Chen and Wowo Ding\*

School of architecture and urban planning, Nanjing University, Nanjing 210093, China; youwei@nju.edu.cn (Y.W.); zhgao@nju.edu.cn (G.Z.); zhchentxy@163.com (C. Z.)

\* Correspondence: dww@nju.edu.cn; Tel.: +96-25-8359-7205

### S1. Grid sensitivity analysis

In the present work, Case A is taken as the example for grid sensitivity analysis. Three grids of Case A are generated by refining and coarsening the basic grid by about a factor 1.5 in each direction, which means a global factor 3.375. The total cell numbers of coarse, basic and fine grid are 1180725, 3938436 and 7387220, respectively. The distributions of wind velocity with three grids are compared along three vertical lines and a central street line, as shown in figure S1. The three vertical lines are at position P1, P2 and P3 and starts from the ground to  $z=30\text{m}$  above the ground. The central street line is at  $z=0.1H$  above the ground. Figure S2 shows the CFD simulation results of wind velocity along the four lines. As shown in figure S2, the wind velocity profiles along the vertical lines respectively show a good agreement (figure S2a-c). However, along the central street line, the profiles of wind velocity calculated with basic grid and fine grid show better agreement (figure S2d). The errors caused by grid resolution have an unnoticeable effect on the numerical results. Therefore, the basic grid resolution applied in this paper is sufficient for numerical simulation.

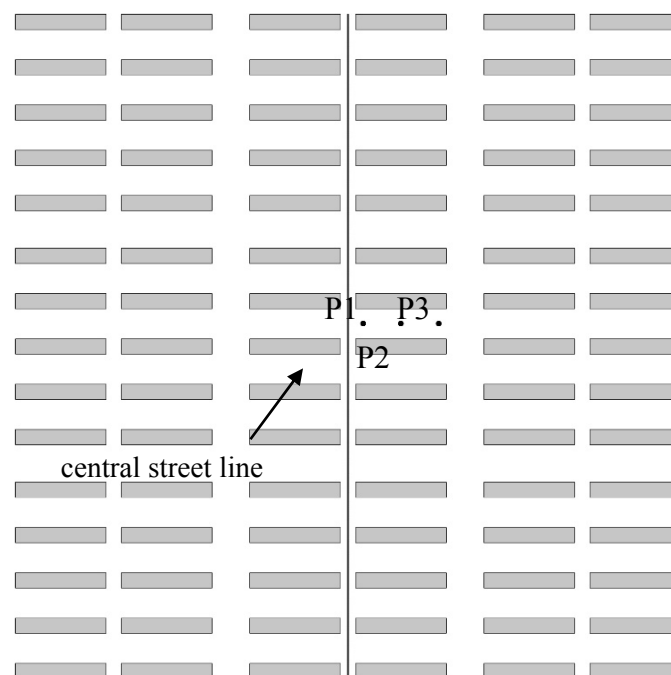


**Figure S1.** Position P1, P2 and P3 of vertical line and central street line located in Case A

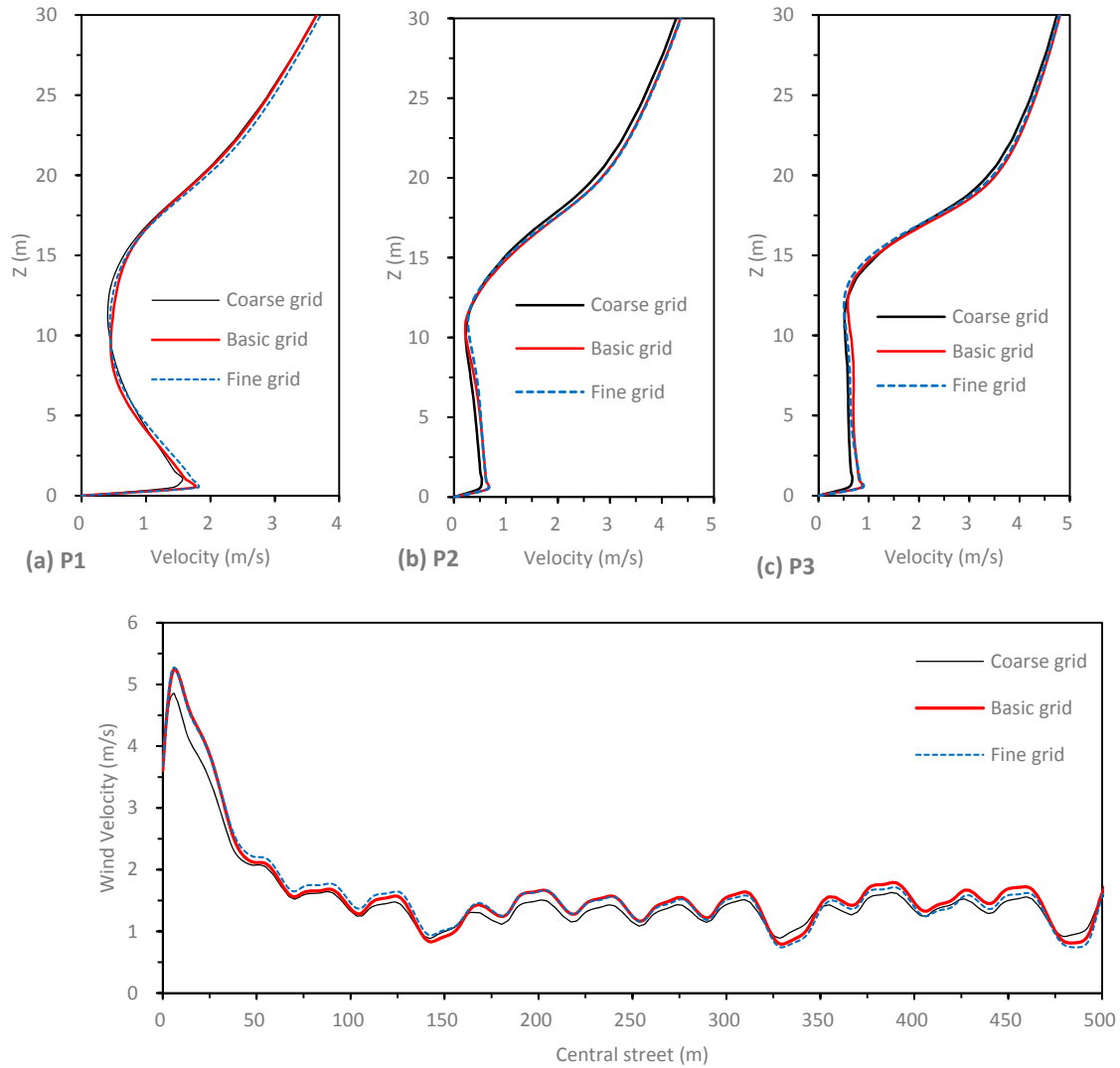


**Figure S2.** The wind velocity profiles along a vertical line at (a) position P1, (b) position P2, (c) position P3, (d) Distribution of wind velocity along the central street line ( $z=0.1H$ ).

**S2. Validation study**

This paper takes the wind-tunnel experiment of strip-type building groups [55] as the validation of CFD simulation. The experiment was carried out in a low-speed wind tunnel at the Hunan University in China. The geometrical model represents a residential area in the South China. Figure S3 shows the tested building arrangement. It consists of some simple rectangular prisms with the same height and width. The side length,  $L_1$ , (building Model 1) is two times  $L_2$  (building Model 2). The aspect ratio of distance  $B_1$ , to the building height  $H$  is set to 1.0. The interval,  $B_2$ , between adjacent two longer side buildings arranged side-by-side is  $0.67H$ . Three typical points are also shown in Figure S3, where the vertical profiles were measured using seven-hole probes. The scale of the experimental model was 1/150 and the experiments were performed only for the S–N wind direction.

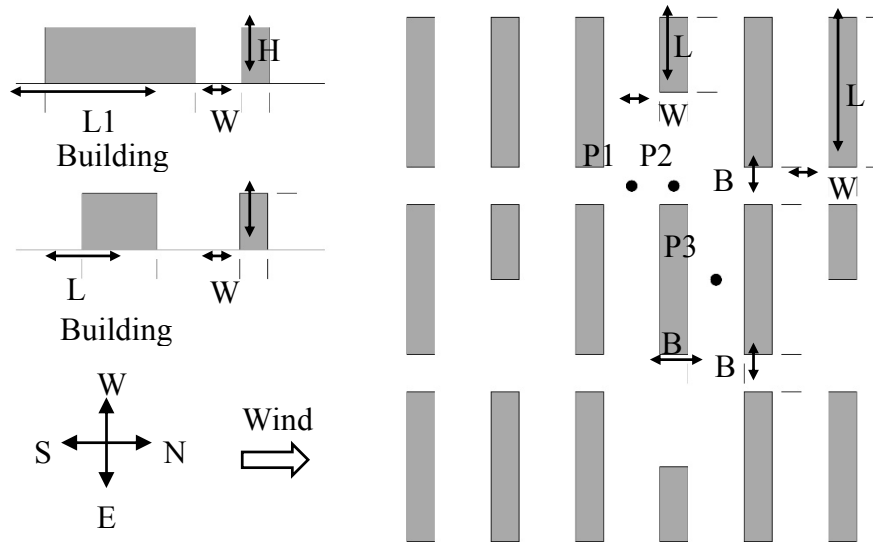


**Figure S3.** Building configurations and arrangements ( $H=18$  m,  $W=9$  m,  $L1=48$  m,  $L2=24$  m):

To better compare CFD simulation results with the wind-tunnel experiment, the CFD simulation was also carried out in 1:150 scale. The computational domain and grid resolution were all in accord with the computational settings in section 4. Figure S4 and S5 shows the computational domain and grid resolution. The lateral and inflow boundaries are set to  $5H$  away from the building groups, where  $H$  is the uniform building height. The outflow boundary is  $20H$  away from the building groups and the height of the computational domain is  $11H$ . The computational domain was also built using hexahedral elements (about 0.94 million). the minimum grid control in direction  $z$  is  $0.028H$ , the minimum grid control in direction  $x$ - $y$  is  $0.056H$ , and the maximum expansion factor between grids is below 1.25.

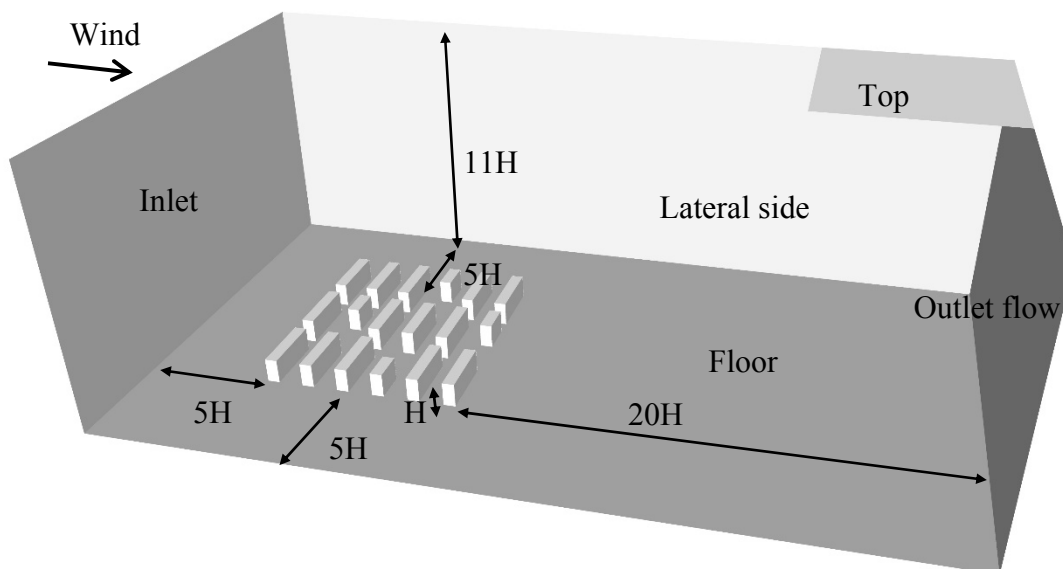


**Figure S4.** (a) Computational domain

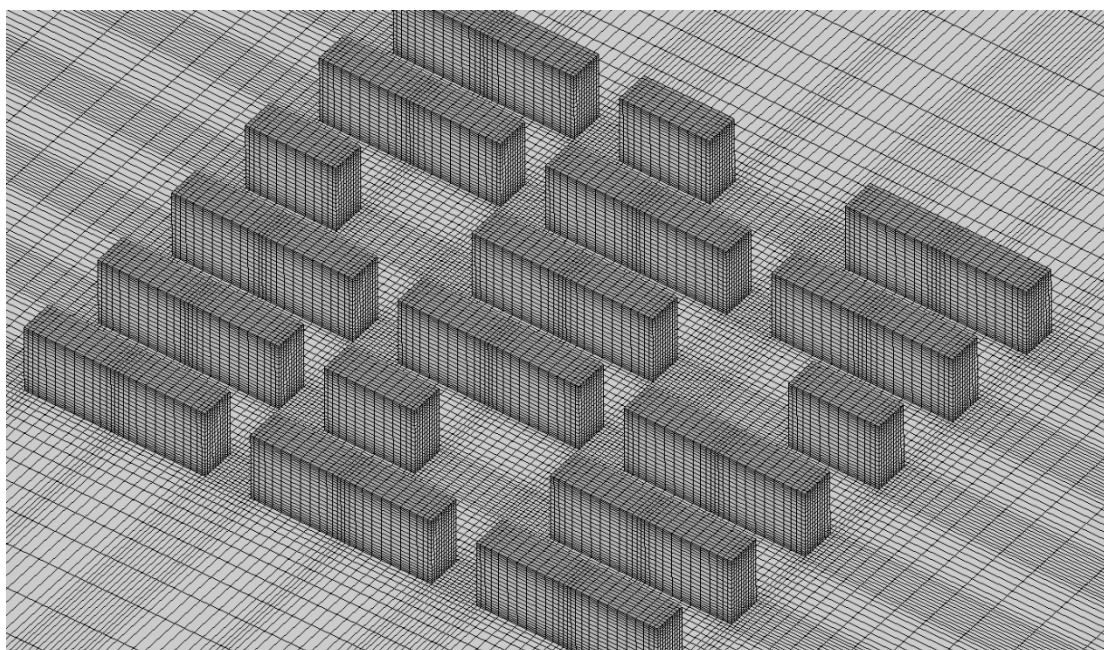


**Figure S5.** Grid resolution in the computational domain

Symmetry boundary conditions were imposed on the top and lateral sides of the domain. At the outlet boundary of the domain a pressure-outlet condition was used. No-slip wall boundary condition was used at all solid surfaces. These boundary conditions were all in accord with the computational settings in section 4. As for the inlet boundary condition, a power-law velocity profile was also applied, but the atmospheric boundary is different with that in our ventilation performance study. In order to compare the numerical results with the experimental quantities, the inlet boundary condition is set according to the experiment. The reference velocity  $U(z)$  is set to be 4.5 m/s at the elevation  $Z = 10$  m. The exponent  $\alpha$  is 0.22 obtained from the experiment. The solver settings are summarized in Table S1.

**Table S1:** The calculation conditions utilized in CFD simulation.

Calculation conditions	Solver settings
Computational domain	2.32m*3.96*1.32m (1:150);
Grid resolution	940,672 hexahedral cells;
Turbulence model	Standard k- $\epsilon$ turbulence model;
Algorithm for pressure-velocity	SIMPLE;
Scheme for advection terms	Second-order discretization for convection terms and the viscous terms;
Boundary conditions	Inflow: According to wind-tunnel experiment; Outflow: pressure-outlet condition; Ground and block surfaces: Non-slip wall; Top and lateral surfaces: Symmetry;
Convergence residual	1e-5

Fig. S6 compares the numerical and experimental results of the measuring points at locations. From the figure, it can be seen that the numerical predictions overall are in satisfactory agreement with the experimental results, especially for the wind profile at position P1 and P2 (Figure S6a-b). The CFD simulation result of wind profile at position P3 is a little lower than experimental results. These measurement points are in location of highly complex recirculating flow regions. This finding agrees with the literature [19,52,54], which indicates that in the wake region behind the building, the

predicted wind speed is generally underestimated. Some papers [35] indicate that this underestimations in the wake region are attributed to the underestimation of turbulent kinetic energy in the wake region, as steady RANS is limited in reproducing the vortex shedding in the wake of buildings. what's more, some errors also come from experimental tests, which are due to measuring device limitations. But overall, the CFD simulation results have a good agreement with experimental results.

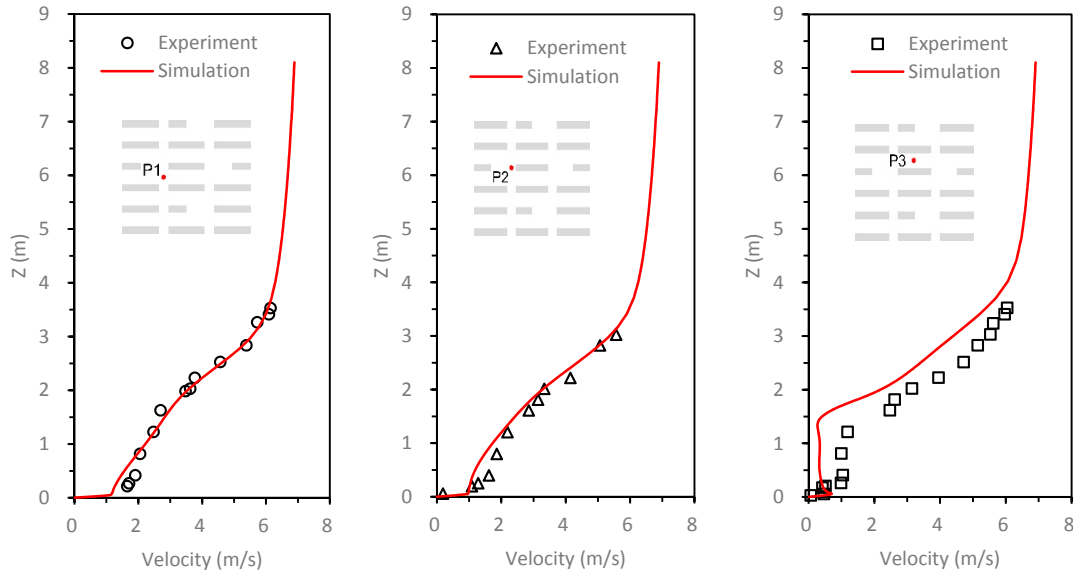


**Figure S6.** Comparison of the numerical and experimental results at (a) position P1, (b) position P2, (c) position P3.

© 2017 by the authors. Submitted for possible open access publication under the terms and conditions of the Creative Commons Attribution (CC BY) license (<http://creativecommons.org/licenses/by/4.0/>).

